FINAL REPORT TO SPONSOR


# Characterization of $Nb_3Sn$ Strand for ITER


Interagency Agreement No. DE-AI05-07OR23274


Prepared for:

US ITER Project Office
Oak Ridge National Laboratory
1055 Commerce Park Dr.
Oak Ridge, TN  37831


Principal Investigators:

Najib Cheggour
Loren F. Goodrich
Electromagnetics Division
Physical Measurement Laboratory
National Institute of Standards and Technology (NIST)
Boulder, Colorado  80305-3337
Phone: 303-497-3143
Fax: 303-497-7364
E-mail: goodrich@boulder.nist.gov

Project/Task 8183440-000 and 8183441-000

May 2012

# FINAL REPORT

# CHARACTERIZATION OF NB₃SN STRAND FOR ITER

**N. Cheggour, L. F. Goodrich, T. C. Stauffer,
B. J. Filla, J. D. Splett, and C. C. Clickner**

**National Institute of Standards and Technology
Boulder, CO 80305**

***Summary***

This final report covers funding from fiscal years 2007 to 2009 with the three year interagency agreement ending 3/31/2010. The total funding was $149,000 for FY2007, $0 for FY2008, and $5,250 for FY2009.

# SUMMARY OF FY 2007 ELECTROMECHANICAL RESEARCH FOR DOE/ITER PROGRAM

## N. Cheggour, L. F. Goodrich, T. C. Stauffer, B. J. Filla, J. D. Splett, and C. C. Clickner

## National Institute of Standards and Technology
## Boulder, CO 80305

## Introduction

We have an ongoing research program for characterization of superconductor composite strands, the principal output of which is sensitive measurements of critical current $I_c$ over a broad range of the essential parameters: longitudinal strain $\varepsilon$, temperature $T$, and magnetic field $B$. This features a new apparatus for integrated measurement of $I_c(\varepsilon,T,B)$ on the same, long-conductor sample without remounting.

This year, we focused most of our effort toward finishing the design, construction, and commissioning of a new variable-strain/variable-temperature apparatus. This facility was used immediately and extensively to characterize a number of $Nb_3Sn$ ITER wires from Luvata and Oxford Superconductor Technology (OST), which yielded important results regarding the influence of heat-treatment on the irreversible strain limit, one of the most critical parameter for electromechanical performance of ITER wires. We also characterized the dependence of critical-current on strain and magnetic field at liquid-helium temperature on Luvata and OST wires for selective heat-treatment schedules, ahead of the tests to be made on the US cables at the SULTAN facility in March 2008.

Several papers were presented this year at various meetings and international conferences. We contributed to the presentations of Dr. John Miller at the ITER conductor meeting held in Villigen (Switzerland) in July 2007, and at the MT-20 conference held in Philadelphia in August 2007. We also presented in great detail the results obtained on ITER conductors at the MEM'07 workshop in Princeton, MT-20 conference in Philadelphia, and the annual Low-Temperature Superconductor workshop (LTSW'07) in Lake Tahoe. We received a very positive feedback on our irreversible-strain-limit study from the ITER community, especially the International Organization (ITER IO). The timing of this study was perceived by this community as being very good, since ITER IO is trying to make hard decisions regarding heat-treatment schedules for toroidal-field (TF) coils.

It is also worth mentioning that, in light of the valuable results we obtained regarding the effect of the heat-treatment on the irreversible strain limit of both OST and Luvata wires, OST changed the design of their ITER strands in order to improve the electromechanical performance. They also recently solicited us to study the effect of the new architecture on the wire electromechanical properties.

Our electromechanical testing program is conducted in a collaborative effort with superconductor manufacturing industries, national laboratories, and universities. Work is planned in consultation with the wire manufacturers and a number of research collaborators within the DOE/OFES (ITER), DOE/HEP (High Energy Physics), and DOE/OE (Office of Electricity) communities. Direct feedback is given

to the wire manufacturers within each project and then disseminated to the general wire-development community.

A brief summary of the results obtained during FY 2007 is given below.

# 1. New variable strain/temperature/magnetic-field apparatus

We finished the construction of the unified apparatus. This new facility combines world-class capabilities in variable-strain and variable-temperature measurements. All the parts of the new facility were designed and built. The apparatus was commissioned, calibrated, and tested (the variable-temperature part of this apparatus will be commissioned in the near future). It has been extensively and successfully used to determine the irreversible strain limit of Luvata and OST $Nb_3Sn$ strands. In addition, $I_c(\varepsilon, B)$ measurements have been made on Luvata and OST strands over a wide range of strain and magnetic field at liquid-helium temperature.



**Figure 1: Photograph of the upper part of the new high-current apparatus constructed at NIST to measure the critical-current dependence on strain, temperature and magnetic field. The worm-wheel that torques the spring can be seen through one of the windows.**

*Application of strain*:

The principle of applying strain to the sample follows the design developed by Walters *et al.* in 1986. The superconducting wire or tape to be investigated is soldered to a thick coiled spring. The spring we have designed is made of the 2% beryllium doped copper alloy ("Alloy 25"). It is attached at its top end to a stainless steel tube (inner shaft) and has its bottom end locked by an outer can. The latter, also made of stainless steel, is firmly fastened to the bottom of the probe, while the inner shaft is connected at its top end to a worm-wheel gear system located at the head of the probe (Fig. 1). Turning the gear worm rotates the inner shaft, which transmits a torque to the

spring. This generates an angular displacement between the spring ends. Depending on the sense of rotation, the sample is put under either a tensile or a compressive strain. To measure the angle of twist applied to the spring, two pointers are attached to the spring ends. The top end of the spring is connected to a thin-walled, long stainless steel tube (outer pointer), while the bottom end is attached to a long rod (inner pointer). Both pointers are located inside the inner shaft and emerge at the head of the probe (Fig. 1). A needle and needle support are attached to the inner pointer. A disk-shaped protractor, made of aluminum, is fastened to the outer pointer. When a torque is applied, the position of the needle relative to the protractor allows the measurement of the angle of rotation of the outer pointer with respect to the inner one. From the reading of the angle of twist ($\theta$), the value of strain applied to the sample can be derived. The exact relationship between $\varepsilon$ and $\theta$ is determined by calibrating the spring using strain gauges.

We used two different designs for the springs: rectangular-section and T-section geometries (Fig. 2). The rectangular-section spring has a relatively large width (4.8 mm) to allow measurements on tape samples, but it is elastic only between -0.7 % and +0.7 %. The T-section spring has a narrow width (2 mm) that can accommodate wires of up to 1 mm in diameter, but it can be elastic over a significantly wider strain range (between -1 % and +1 %). The elastic strain range very much depends on the design parameters and the spring material.



**Figure 2: Photograph of the two CuBe springs used in the new high-current apparatus: rectangular-section (top) and T-section (bottom) geometries.**

*Spring calibration*:

The springs were calibrated to measure the strain-angle relationship. Several strain gauges were glued to the outer surface of each spring (Fig. 3). To check the effect of temperature, the calibration was performed at room temperature, 76 K and 4 K. The longitudinal strain varies linearly as a function of the angle of twist for both compressive and tensile strain regimes (Fig. 3). As expected from design calculations, strain is reversible within the strain window from -0.7 % to +0.7 % for the rectangular-section spring, and within the strain window from -1 % to +1 % for the T-section spring. Furthermore, calibrations performed at variable temperatures show

that the calibration factor is temperature-independent to better than 3 % between room temperature and 4 K, and better than 1 % between 76 K and 4 K.
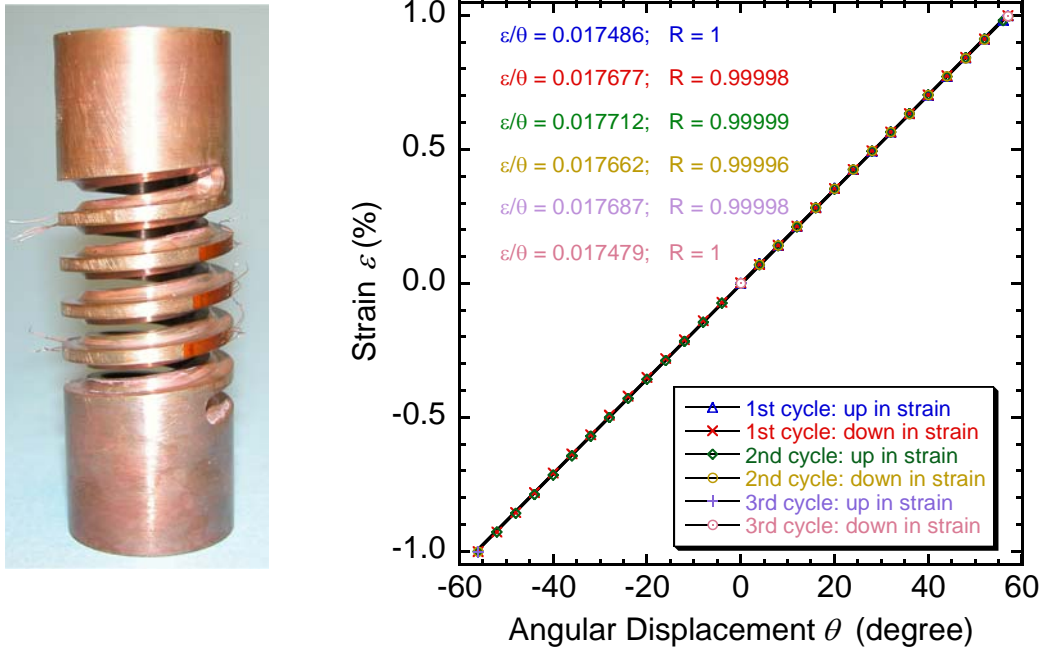


**Figure 3: Calibration results for the T-section, CuBe spring.**

The spring has 4 active turns. Figure 4 shows a T-section spring with a helical $Nb_3Sn$ sample soldered to it. We attach 3 pairs of voltage taps to the sample along the central three turns of the spring, each cover one turn (about 8 cm long). This relatively long separation of voltage taps allows for critical-current measurements at electric-field criteria as low as 0.01 µV/cm. We typically measure critical currents over a range of electric-field criteria from 0.01 to 1.0 µV/cm (1 to 100 µV/m). We chose to use three pairs of voltage taps in order to substantially improve the statistics of our measurements. This is especially important for the determination of the irreversible strain limit since this allowed us to get three separate determinations from each specimen. Our data acquisition system uses three nano-voltmeters to measure these three taps simultaneously.
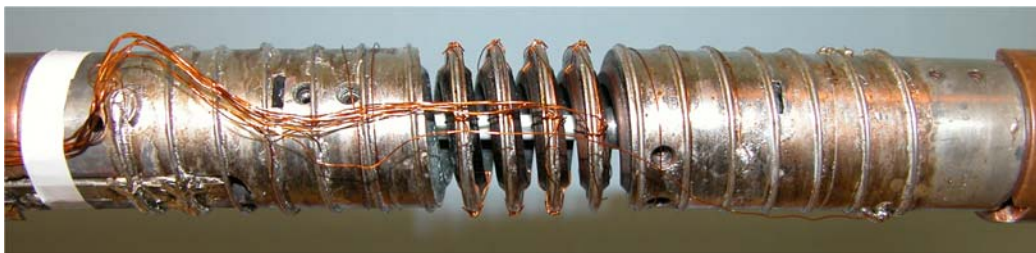


**Figure 4: Photograph of a T-section, CuBe spring with a helical sample soldered to the spring. Three pairs of voltage taps cover the three central turns of the spring. The current contacts are made at each end of the spring.**

4

## 2. Critical current measurements

We were invited to participate in an interlaboratory comparison of routine critical-current measurements using a well characterized CERN Nb-Ti wire. This comparison is being headed by Lawrence Berkley National lab (LBNL). We made measurements at 4, 5, 6, 7, 8, and 9 T at 4.2 K with the NbTi sample mounted to our T-section, CuBe spring. Our measurements were in good agreement with those of the other laboratories participating to this interlaboratory comparison (Fermi lab, Brookhaven National lab, Lawrence Berkley National lab, and Florida State University). An abstract on this comparison was submitted for ASC'08. We also made critical-current measurements on this NbTi wire as a function of strain using the new spring apparatus. These results indicate that the effect of longitudinal and bending strain do change the measured critical-current by a non-negligible amount.

We have begun software development for automation of $I_c(\varepsilon,T,B)$ measurements. Some level of automation is absolutely essential for this research and we needed to start software development early in this project. Further development of more advanced automation is expected to help maintain data reliability and increase the number of samples that we can fully characterize per year. The acquisition needs to be robust to run through a sequence of measurements with minimum human input. The computer programs are expected to be very specialized for our systems and evolve at least over the next few years.

The compounding of all three variables $(\varepsilon,T,B)$ makes an already labor- and time-intensive characterization very formidable; however, the results cannot be generated any other way and are needed to answer key questions about strain and temperature safety margins for ITER giant magnets. Full characterization of a single sample is expected to require two to three months of intensive work and significant consumption of liquid helium. Currently, the community perception is that every $Nb_3Sn$ conductor needs to be fully characterized due to the lack of consensus on unified scaling and due to the larger extrapolations needed for some new systems. We hope that our future data will be a basis for consensus on unified scaling and/or will define the limits to scaling. Unified scaling is expected to allow for more precise estimations of conductor performance over a wide range of parameters using a more limited and cost-effective data set.

We have used Basic for instrument control and data acquisition and analysis for about 25 years. For this program, we have decided to switch to LabVIEW programs that will run on one computer with fewer instruments, new predictive algorithms, and new control signals for more robust operation. We also need the program to use multiple acquisition modalities to accommodate various sample properties while maintaining accuracy and efficiency.

Figure 5 shows a screen capture of our critical-current data acquisition and analysis program. There are 12 different tabs (screens) in our new LabVIEW program that include initialization, run matrix (strain, temperature, and field points), displays, results, run time data, advanced controls, system state, and stability stats. The plot on the left shows $I_c(\varepsilon)$ at 12 T with loaded and unloaded points for each of the three voltage taps. On the right are full-logarithmic plots of $E$-$I$ for each of the three regions of the sample. The lower plot shows the raw $E$-$I$ points and the upper plot shows critical current values at various criteria. These run-time displays give the operator feedback on the relative consistency of the three sample regions, the location of the peak critical current, and where the strain effect becomes irreversible. Other run-time displays show sample voltage and current readings as a function of time and

voltage drops over various portions of the sample current path including each end of the sample and the current contacts to the sample.
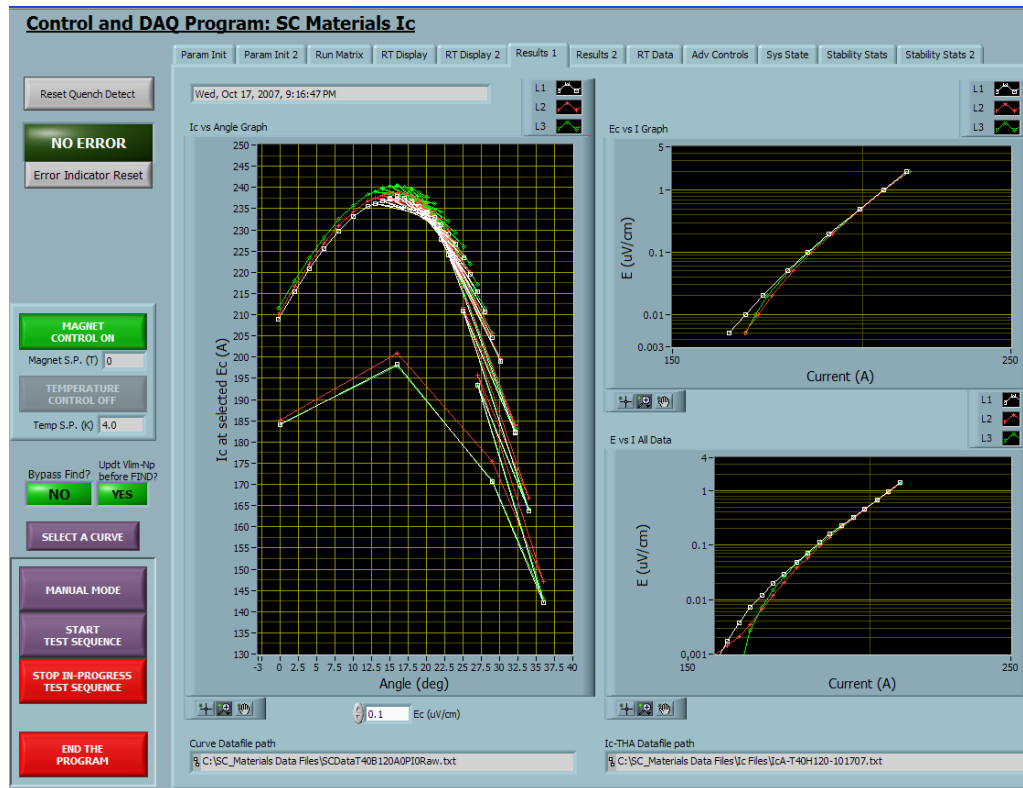


**Figure 5: Screen capture of the front panel of LabVIEW critical-current data acquisition and analysis program developed at NIST. There are 12 different tabs (screens) that include initialization, run matrix (strain, temperature, field), displays, results, run time data, advanced controls, system state, and stability stats.**

## 3. Irreversible-strain-limit measurements

For a given wire, the dependence of the critical current on strain is reversible within a certain strain limit. Beyond this limit (irreversible strain limit, $\varepsilon_{irr}$), the wire is damaged due to crack formation in the superconductor and its critical current is significantly lower. Our first set of measurements with the new apparatus was to determine the irreversible strain limit of Luvata and OST baseline and alternate design $Nb_3Sn$ ITER strands. These measurements were made as a function of strain at 12 T and 4 K, $I_c$ ($B = 12$ T, $T = 4$ K, $\varepsilon$). Strain was loaded and unloaded to determine the irreversible strain limit. The hypothesis is that more aggressive (higher temperature and/or longer time) heat treatments can cause the $Nb_3Sn$ filaments to grow together, which would decrease the irreversible strain limit of the wire. The filament design of the wire will also affect the sensitivity of the irreversible strain limit to the heat treatment parameters.

A total number of 28 specimens were measured at 4 K and 12 T to determine the effect of the heat treatment on irreversible strain limit. We have observed different behaviors between Luvata and OST wires:

6

## Luvata Nb$_3$Sn strands

We investigated 2 strands from Luvata with diameters of 0.818 mm (baseline design) and 0.773 mm (alternate design). Each of the Luvata wires received three heat-treatments at 650 ˚C: Short (100 hours); intermediate (175 hours); and long (240 hours). For each wire and heat-treatment schedule, we measured two to four specimens. This, combined with the fact that we measure three segments of each sample, gave us very good statistics for determining the irreversible strain limit. Some examples of the results obtained are illustrated in Figs. 6a-6c, and a grand summary is shown in Table 1. Each of the numbers for $\varepsilon_{irr}$ (and $I_{cmax}$) given in Table 1 are averages of the results obtained on six to twelve wire segments (each about 8 cm long). Data obtained when a sample was loaded and unloaded are respectively labeled with unprimed and primed letters and represented with solid and open symbols in Figs. 6a-6c. The irreversible strain limit $\varepsilon_{irr}$ corresponds to the strain at which the first drop of unloaded points from the original $I_c(\varepsilon)$ curve occurs, interpreted as the onset of crack formation in the Nb$_3$Sn brittle filaments. The compressive pre-strain $\varepsilon_{max}$ stems from the differential thermal contraction among the conductor components. Finally, the intrinsic irreversible strain limit, reported in Tables 1 and 2, corresponds to $\varepsilon_{irr,\,0} = \varepsilon_{irr} - \varepsilon_{max}$.
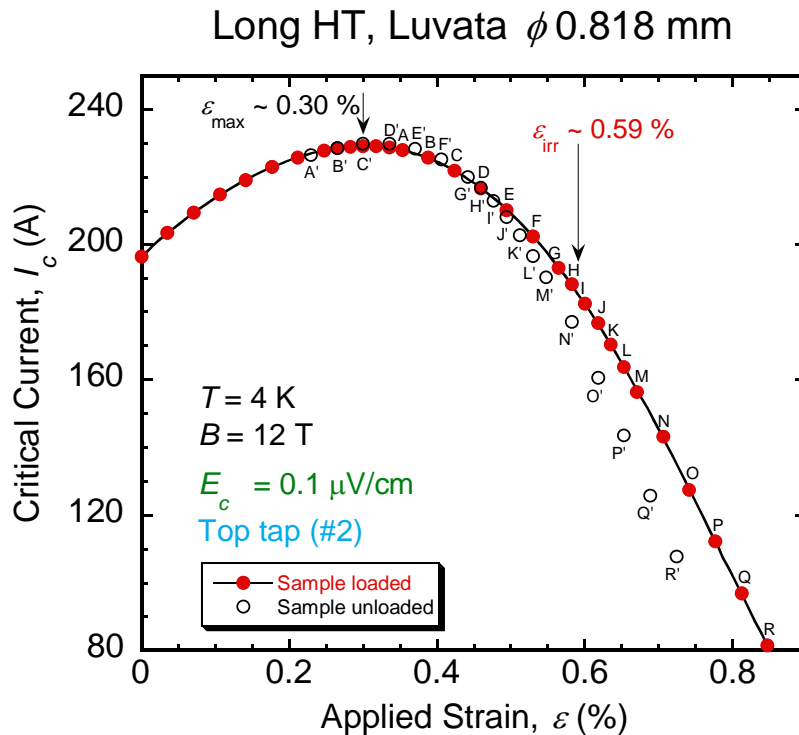


**Figure 6a: Critical-current versus tensile strain for a Luvata Nb$_3$Sn ITER wire (baseline design), heat-treated at 650 ˚C for 240 hours. The irreversible strain limit $\varepsilon_{irr}$ is about 0.59 %.**
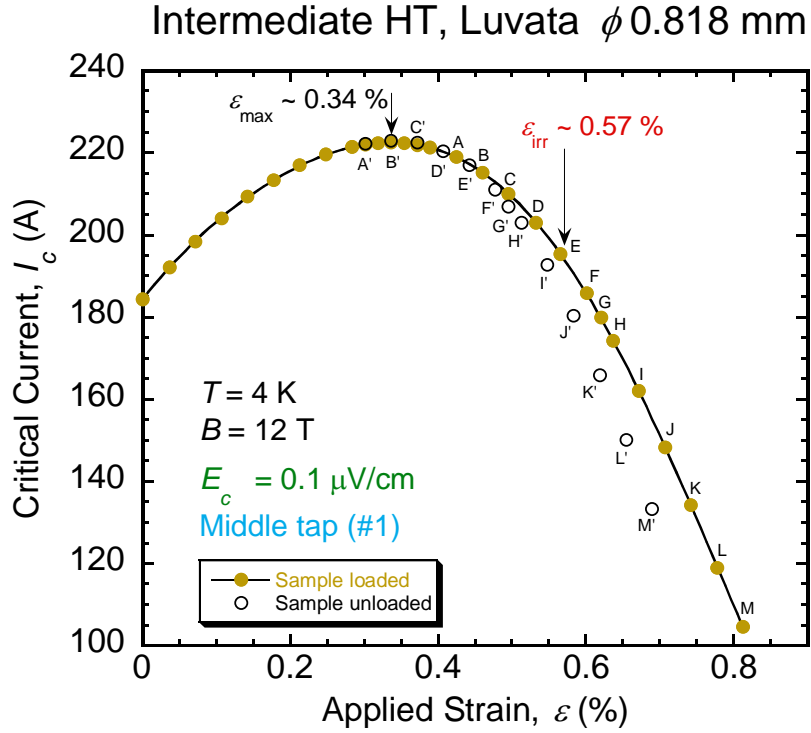
**Figure 6b:** Critical-current versus tensile strain for a Luvata Nb₃Sn ITER wire (baseline design), heat-treated at 650 ˚C for 175 hours. The irreversible strain limit $\varepsilon_{irr}$ is about 0.57 %.
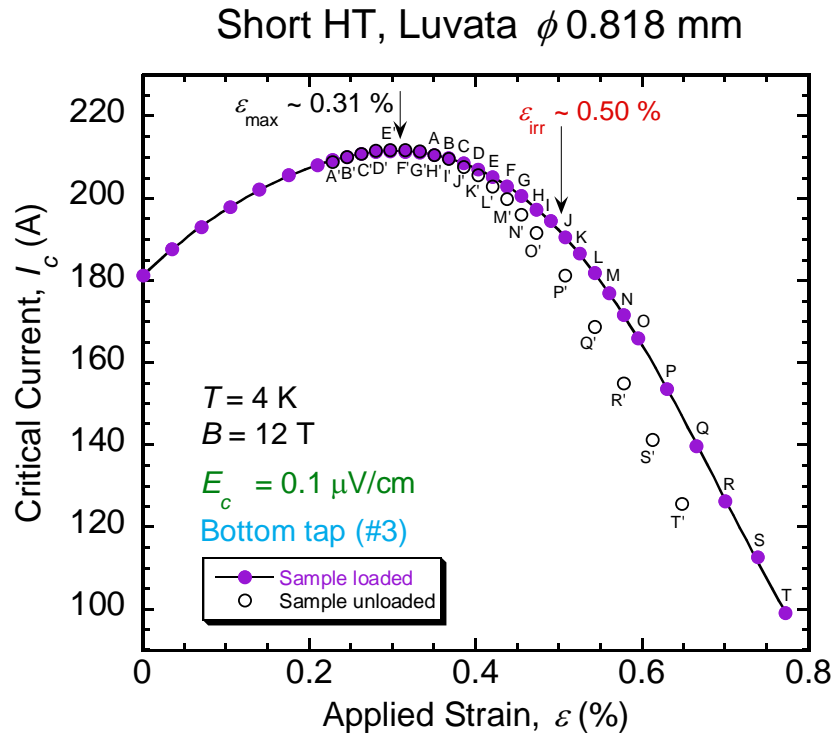


**Figure 6c:** Critical-current versus tensile strain for a Luvata Nb₃Sn ITER wire (baseline design), heat-treated at 650 ˚C for 100 hours. The irreversible strain limit $\varepsilon_{irr}$ is only about 0.50 %.

Our results show that the irreversible strain limit actually increases with the heat treatment time, contrary to our initial hypothesis, at least for these Luvata conductors (Figs. 6a-6c, Table 1). We believe that the explanation of this can be linked to the micro-structural observations made by the Florida State University (M. Jewell *et al*.) where they showed in heavily deformed samples that $Nb_3Sn$ filaments with unreacted Nb cores at the center are more likely to have longitudinal cracks. Micrographs of Luvata wires showed the presence of such unreacted cores for specimens which received the short heat-treatment (Fig. 7a). These unreacted Nb cores were also shown to greatly decrease in number for specimens that received the intermediate or the long heat-treatment (Fig. 7b). From these micrographs and the $\varepsilon_{irr}$ data obtained, we can conclude that unreacted Nb cores may indeed promote early filament breakage, consistent with Jewell *et al.* microstructural observations. Therefore, the presence of un-reacted Nb cores seems to be one important factor in determining the irreversible strain limit of $Nb_3Sn$ wires.

Our results also showed that the irreversible strain limit is a function of the electric-field criterion that is used to determine the critical current. The critical currents at lower criteria appear to be more sensitive to the first filament cracking and thus, lower criteria yield lower estimates for the irreversible strain limit (Table 1). Hence we suggest using the lowest criterion possible in order to obtain an irreversible strain limit that closely corresponds to the first filament cracking of the wire being measured.

We also measured ac-losses in magnetic field between ±3 T in order to determine if long heat-treatment times result in bridging of the $Nb_3Sn$ filaments (non-copper ac-losses are included in Table 1). There seem to be a moderate increase in ac-losses by about 12 % between the long and short heat-treatment for the baseline wire design, and a substantial increase of about 39 % for the alternate wire design. The increase in $I_c$ between the two heat-treatments was 6 % and 22 %, respectively, which accounts for at least half of the ac-loss increase in both cases. Therefore, the ac-loss increase is not predominantly caused by filament bridging. The micrograph in Fig 7b shows that filament bridging is rather limited, which confirms this point.

## Intrinsic irreversible strain limit: Summary for Luvata strands

| | $\varepsilon_{irr,0}$ (%) | $\varepsilon_{irr,0}$ (%) | $\varepsilon_{irr,0}$ (%) | ac-losses (mJ/cm$^3$) | $I_{c,max}$ (A) |
|---|---|---|---|---|---|
| $E_c$ (µV/cm) | 0.01 | 0.1 | 1 | | 0.1 |
| Short HT; 0.773 mm | 0.13 | 0.15 | 0.17 | 246 | 162 |
| Intermediate HT; 0.773 mm | 0.31 | 0.33 | 0.38 | 327 | 193 |
| Long HT; 0.773 mm | 0.30 | 0.33 | 0.37 | 342 | 198 |
| Short HT; 0.818 mm | 0.19 | 0.19 | 0.23 | 302 | 214 |
| Intermediate HT; 0.818 mm | 0.22 | 0.25 | 0.29 | 313 | 223 |
| Long HT; 0.818 mm | 0.25 | 0.28 | 0.32 | 337 | 226 |

**Table 1: Effect of the heat-treatment schedule on the intrinsic irreversible strain limit $\varepsilon_{irr,0}$. Summary of the data obtained for the Luvata baseline and alternate ITER wire designs. We determined the critical current at the criteria of 0.01 µV/cm, 0.1 µV/cm, and 1.0 µV/cm.**

**Figure 7a: Micrograph of an unstrained Luvata ITER wire reacted at 650 ˙C for 100 hours (Short HT). There is a significant number of unreacted cores inside the filaments. These unreacted cores are believed to act as crack initiators (M. Jewell et al., Florida State University). Image courtesy of T. Pyon, Luvata Waterbury Inc.**
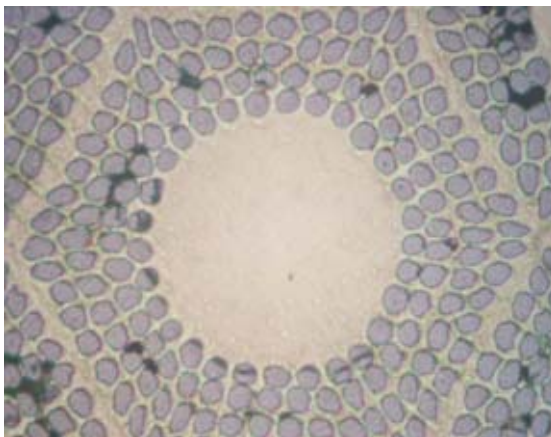


**Figure 7b: Micrograph of an unstrained Luvata ITER wire reacted at 650 ˙C for 240 hours (Long HT). There are very few unreacted cores inside the filaments. Image courtesy of T. Pyon, Luvata Waterbury Inc.**

## OST Nb$_3$Sn strands

A study similar to that completed for Luvata strands was carried out on OST ITER Nb$_3$Sn wires. The irreversible strain limit was determined for a matrix of 12 samples. We investigated 3 strands from OST with diameters of 0.817 mm (baseline design) and 0.772 mm (alternate design). One of the 3 strands was reinforced with Glidcop (wire diameter 0.817 mm). The OST wires without Glidcop received two heat-treatments at 650 ˙C: Short (100 hours), and long (200 hours). The reinforced wire received the short heat treatment (100 hours). These critical-current measurements were made as a function of strain at one field and one temperature, $I_c(B$=12 T, $T$=4 K, ε). The strain was loaded and unloaded to determine the irreversible strain limit, in the same fashion as described above for Luvata samples.

Unlike Luvata wires, our results showed that the irreversible strain limit of OST wires remained the same for the long heat-treatment in comparison to the short heat-treatment (Figs. 8a-8c, Table 2), even though micrographs of OST strands showed that the unreacted Nb cores tend to disappear with the long heat-treatment, in very much the same way as Luvata wires (Fig. 9). However, whereas unreacted cores disappeared with the long heat-treatment of OST wires, a substantial filament bridging took place at the same time (Fig. 9). Indeed, there seem to be a substantial increase in ac-losses by about 30 % between the long and short heat-treatment for the baseline wire design, and about 56 % for the alternate wire design. The increase in $I_c$ between the two heat-treatments was only 10 % and 8 %, respectively, which only represents a small portion of the ac-loss increase in both cases. Therefore, the ac-loss increase is predominantly caused by filament bridging.

We suggest that this filament bridging in OST wires nullified any improvement in the irreversible strain limit that was expected from the reduction of the number of unreacted Nb cores by using long heat-treatment times. This suggestion of filament bridging is substantiated by ac-loss measurements we made on these specimens (Table 2). Data showed more increase in ac-losses between the short and long heat-treatments in the case of OST wires in comparison to Luvata strands, even thought the difference in time between the short and long heat-treatments was more for the Luvata strands.

The results obtained on OST strands highlight another important factor influencing the irreversible strain limit in $Nb_3Sn$ conductors, which is filament bridging.
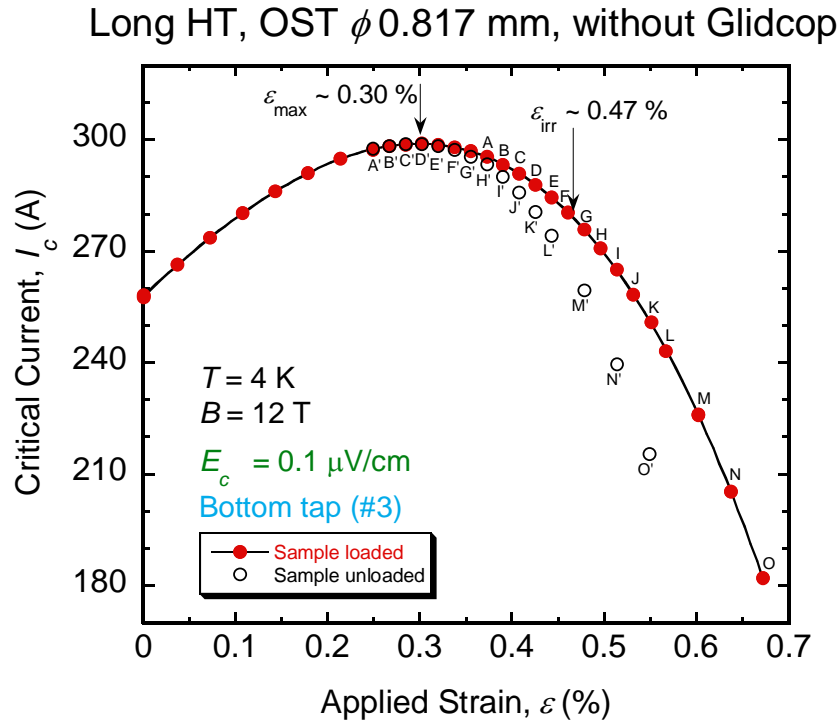


**Figure 8a:** **Critical-current versus tensile strain for an un-reinforced OST Nb₃Sn ITER wire (baseline design), heat-treated at 650 ˚C for 200 hours. The irreversible strain limit $\varepsilon_{irr}$ is about 0.47 %.**
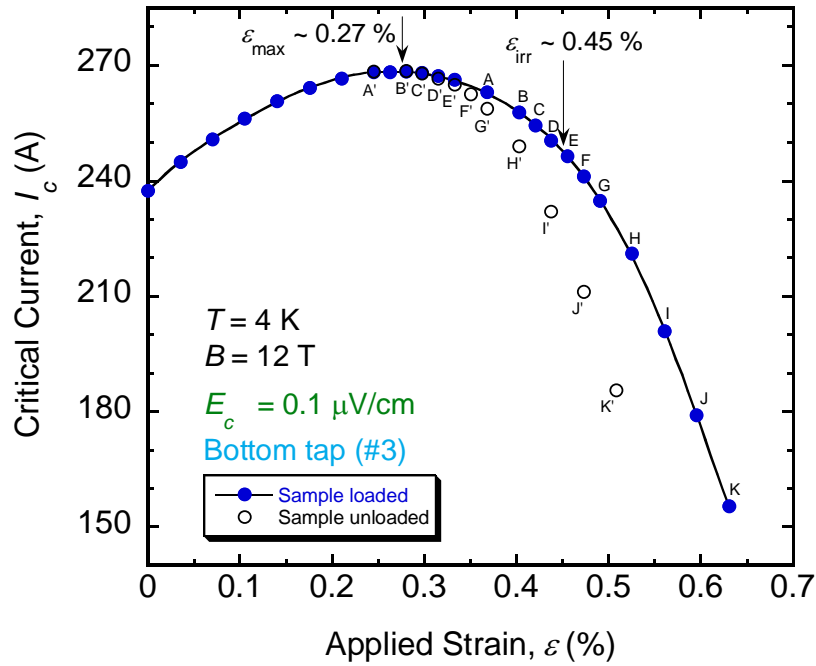
**Figure 8b:** Critical-current versus tensile strain for an un-reinforced OST $Nb_3Sn$ ITER wire (baseline design), heat-treated at 650 °C for 100 hours. The irreversible strain limit $\varepsilon_{irr}$ is also about 0.45 %.
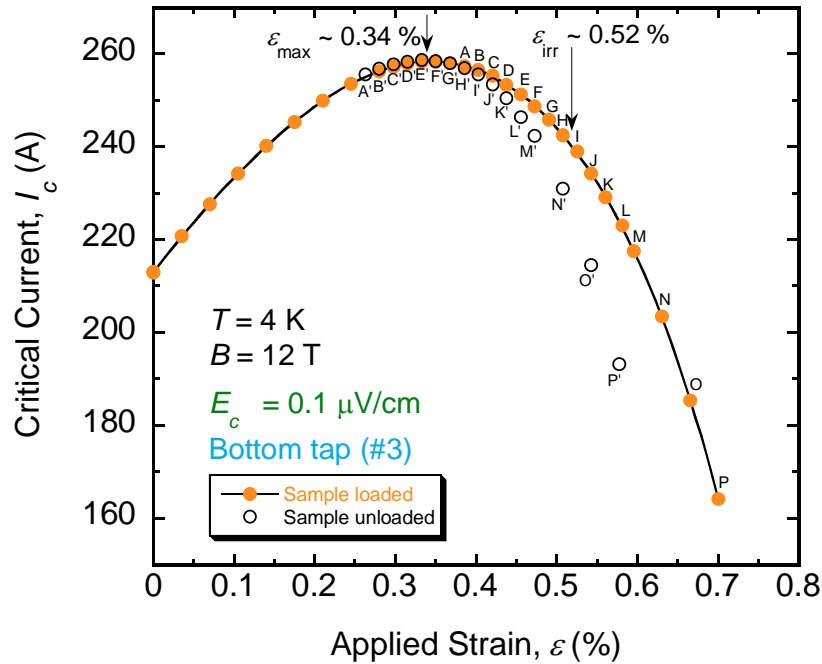


**Figure 8c:** Critical-current versus tensile strain for a Glidcop-reinforced OST $Nb_3Sn$ ITER wire heat-treated at 650 °C for 100 hours. The irreversible strain limit $\varepsilon_{irr}$ is about 0.52 % and the compressive pre-strain $\varepsilon_{max}$ shifted to 0.34 %.

# Intrinsic irreversible strain limit: Summary for OST strands

| | $\varepsilon_{irr,0}$ (%) | (%) | (%) | ac-losses (mJ/cm$^3$) | $I_{c,max}$ (A) |
|---|---|---|---|---|---|
| $E_c$ (µV/cm) | 0.01 | 0.1 | 1 | | 0.1 |
| Short HT; 0.772 mm | 0.16 | 0.19 | 0.22 | 1373 | 221 |
| Long HT; 0.772 mm | 0.18 | 0.19 | 0.21 | 2136 | 238 |
| Short HT; 0.817 mm | 0.14 | 0.17 | 0.23 | 692 | 272 |
| Long HT; 0.817 mm | 0.15 | 0.17 | 0.23 | 897 | 298 |
| Short HT/Glidcop; 0.817 mm | 0.18 | 0.19 | 0.25 | 825 | 255 |

**Table 2: Effect of the heat-treatment schedule on the intrinsic irreversible strain limit $\varepsilon_{irr,0}$. Summary of the data obtained for the OST baseline and alternate ITER wire designs. We determined the critical current at the criteria of 0.01 µV/cm, 0.1 µV/cm, and 1.0 µV/cm.**



B9947 .817mm, ITER 650-100 HT,center hex

B9947 .817mm, ITER 650-100 HT,HP

B9947 .817mm, ITER 650-200 HT,center hex

B9947 .817mm, ITER 650-200 HT, HP
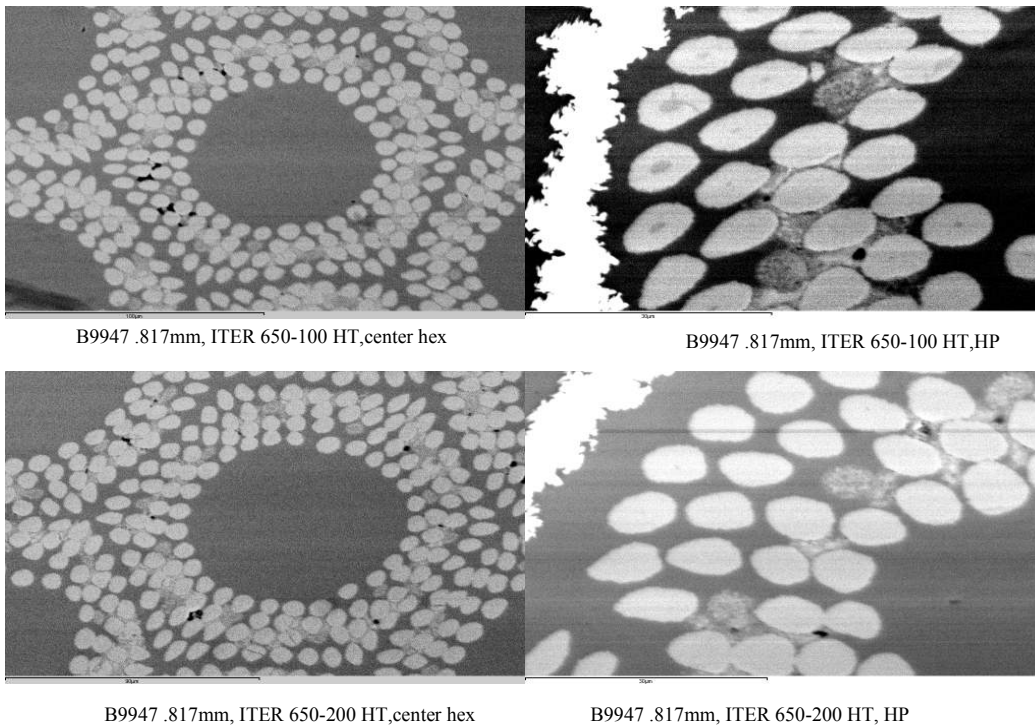
**Figure 9: Micrographs of unstrained OST ITER wires reacted at 650 ˙C for 200 hours (Long HT) and 100 hours (Short HT). Nb unreacted cores tend to disappear with the long HT but, at the same time, filament bridging start to form. Image courtesy of J. Parrell, OST.**

Moreover, there is no substantial difference in the intrinsic irreversible strain limit $\varepsilon_{irr,\,0}$ between the un-reinforced and Glidcop-reinforced OST wires (Table 2). The Glidcop reinforcement was added on the outside of the wire, and hence it is not expected to change the cracking behavior of $Nb_3Sn$ filaments. Glidcop reinforcement, however, increased the wire compressive pre-strain $\varepsilon_{max}$. It is worth mentioning that Glidcop-reinforcement may present an advantage in unsupported cable designs, such as cable-in-conduit conductors (CICC), since the reinforced strand may bend less under the same load conditions due to its improved yield strength.

We would like to remark that the OST alternate wire design we measured here was not the one supplied to US-ITER for making CICC samples (for the SULTAN tests). The wire we measured was not optimized to meet the ITER specifications, as evidenced by its high ac-losses (Table 2).

## 4. Critical-current measurements vs. strain and magnetic field for Luvata and OST Nb$_3$Sn ITER strand*s*

We measured the critical current at 4.0 K, as a function of strain (typically from about -1 % up to the irreversible strain limit), and over a broad range of magnetic fields (up to 16 T). When sample stability and homogeneity were adequate, $I_c(\varepsilon, B)$ measurements were made up to electric currents of about 950 A in liquid helium (Fig. 10a). Our new facility is expected to be the highest-current apparatus of its type in the world and will help answer fundamental questions about the performance of strain-sensitive superconductors.

The relative stability of a superconducting sample during an $I_c$ measurement is not well defined as it depends on many intrinsic as well as extrinsic parameters. The intrinsic parameters include the amount and distribution of the stabilizer, the residual resistivity ratio ($RRR$) of the stabilizer, the effective filament diameter, the $n$-value (steepness of the $V$-$I$ curve), the intrinsic homogeneity of the critical current, and the critical-current density. The extrinsic parameters include damage and strain induced inhomogeneity of $I_c$, contact heating, and sample motion. Often, for a given specimen, the maximum stable voltage $V$ or electric field $E$ will increase with increasing magnetic field, where $I_c$ is lower. The maximum stable $E$ is an indication of the relative stability of the sample during an $I_c$ measurement. In some cases, the $I_c$ criterion of $E = 0.1$ μV/cm (or even 0.01 μV/cm) cannot be achieved at a lower magnetic field for some or all of the three voltage-tap pairs. We would monitor the maximum stable $E$ as a function of magnetic field at a given strain to decide if we should attempt a measurement at a lower field. It is difficult to know whether the intrinsic stability of the wire is limiting the $V$-$I$ curve or whether the extrinsic conditions of the measurement are responsible.

Stability of the measured Luvata wires (Figs. 10a, 10b) was generally better than that of OST strands (Figs. 11a, 11b), as indicated by the maximum stable $E$ during measurements of $V$-$I$ curves. The OST baseline design wire, however, showed a much improved stability behavior at compressive strains. This unexpected improvement allowed us to measure this wire up to high currents of about 900 A at the compressive-strain regime, whereas at the tensile-strain regime, we could not measure it much beyond 500 A due to limited homogeneity and stability (Fig.11a). This interesting behavior is worth investigating further, and may explain why some CICC samples made of OST wires performed very well in SULTAN tests.

We were not able to determine $I_c$ for tap #3 of the measured OST baseline design sample at magnetic fields of 5, 6, and 7 T and strains less than -0.45 % (missing points in Fig. 11a). This was caused by $I_c$ inhomogeneity in this sample that limited the *V-I* data on tap #3 to less than $E_c$ (0.1 µV/cm) for this magnetic field and strain region. The spread in the values of critical current in this region was only about 3 % among the three taps, but the *n*-values were high enough that the lower $I_c$ portion of this sample limited the measured current range for the other taps. This is in contrast to the cause behind the missing points in the tensile-strain regime where little or no voltage was observed on any tap below the quench current. In this tensile-strain regime, the limiting factor in the $I_c$ measurements was predominantly the reduced stability of the wire, rather than $I_c$ inhomogeneity.

Results of $I_c(\varepsilon, B)$ allowed us to verify scaling of the pinning force with magnetic field for the various strain values that were applied to each sample. An example is given in Fig. 12. As evidenced in this figure, the wide range of $I_c$ with the new apparatus allowed measurements over a large portion of the pinning force curve for all applied strains. For each sample, a global fitting of all the pinning-force ($F_p = I_c \times B$) data was obtained using field dependence for $F_p$ of the form:

$$F_p = K b^p (1 - b)^q,\qquad(1)$$

where $b = B/B_{c2}^*$ is the reduced magnetic field, $B_{c2}^*$ is the effective upper critical field at which $F_p$ extrapolates to zero, $p$ and $q$ are constants, and $K$ is an arbitrary function of temperature and strain. The effective upper critical field $B_{c2}^*$ is then fitted using the Durham expression:

$$B_{c2}^* = B_{c2\,\mathrm{max}}^* \left(1 + c_2\varepsilon^2 + c_3\varepsilon^3 + c_4\varepsilon^4\right),\qquad(2)$$

where $B_{c2\,\mathrm{max}}^*$ is the maximum value of $B_{c2}^*$ obtained at the intrinsic strain $\varepsilon = 0$, and $c_2$, $c_3$, and $c_4$ are constants. A list of the fitting parameters obtained for the four wires measured is provided in Table 3.

The dependence of $B_{c2}^*$ on strain is depicted in Fig. 13. Luvata wires seem to be slightly more sensitive to high compressive strain as compared to OST strands. It is known that ternary elements in the composition of $Nb_3Sn$ wires affect their strain sensitivity. We can speculate that these wires may contain different ternary elements, or different effective amounts of the ternary elements in the $Nb_3Sn$.
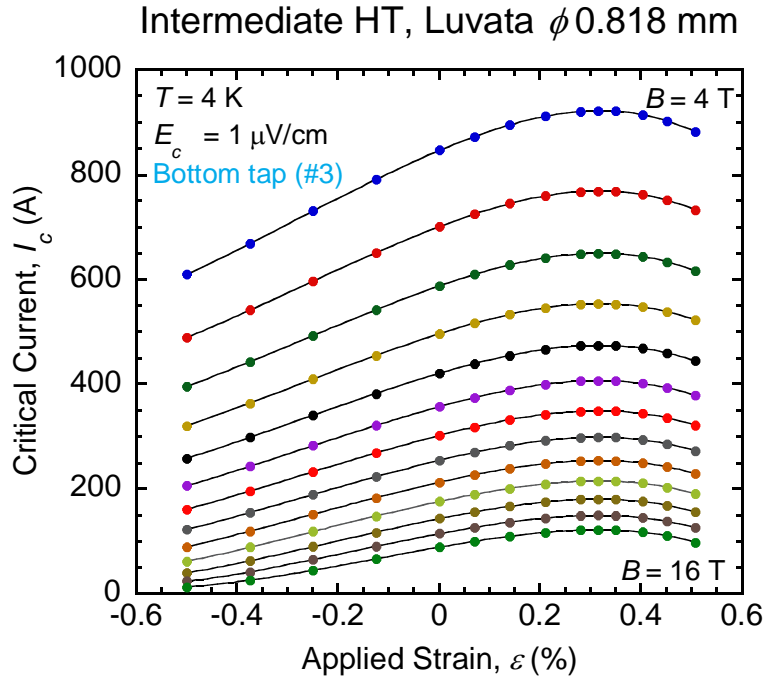
**Figure 10a: Critical-current (at 1 µV/cm) vs. strain and magnetic field for a Luvata Nb₃Sn ITER wire (baseline design), heat-treated at 650 ˙C for 175 hours. Measurements were made up to electric currents of about 950 A in liquid helium.**
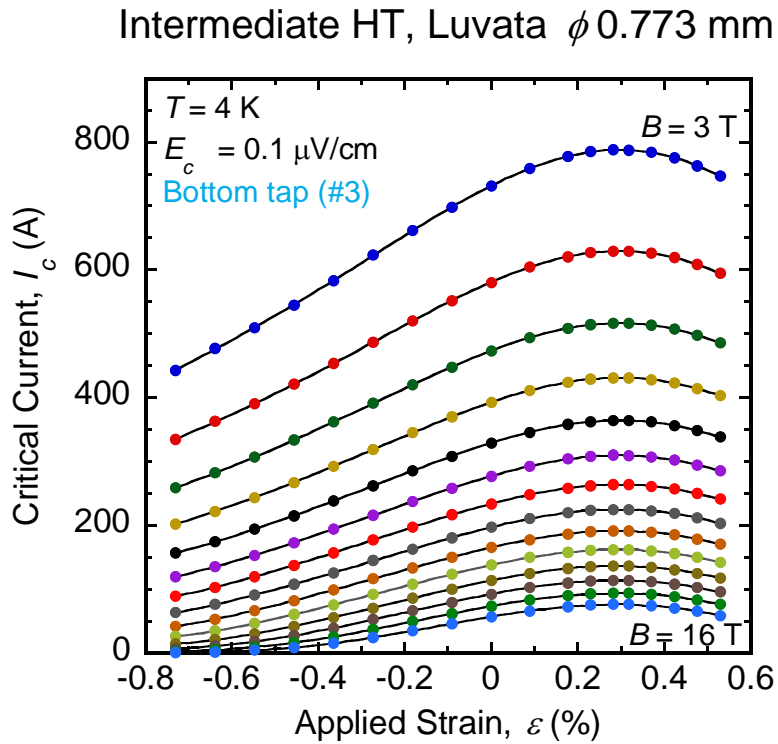


**Figure 10b: Critical-current (at 0.1 µV/cm) vs. strain and magnetic field at 4 K for a Luvata Nb₃Sn ITER wire (alternate design), heat-treated at 650 ˙C for 175 hours.**
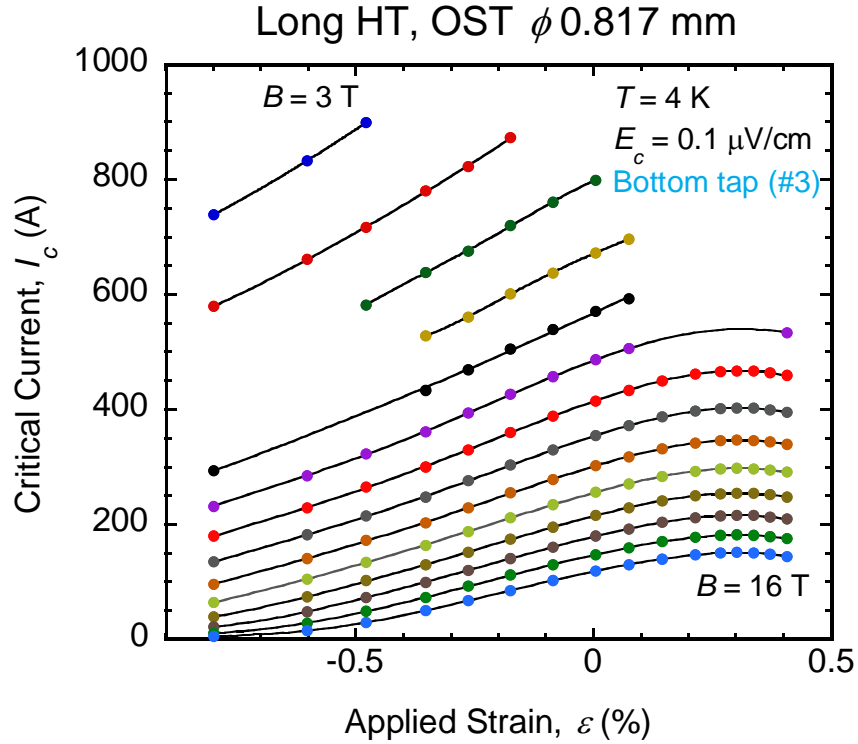
**Figure 11a: Critical-current (at 0.1 μV/cm) vs. strain and magnetic field at 4 K for an OST Nb₃Sn ITER wire (baseline design), heat-treated at 650 ˙C for 200 hours.**
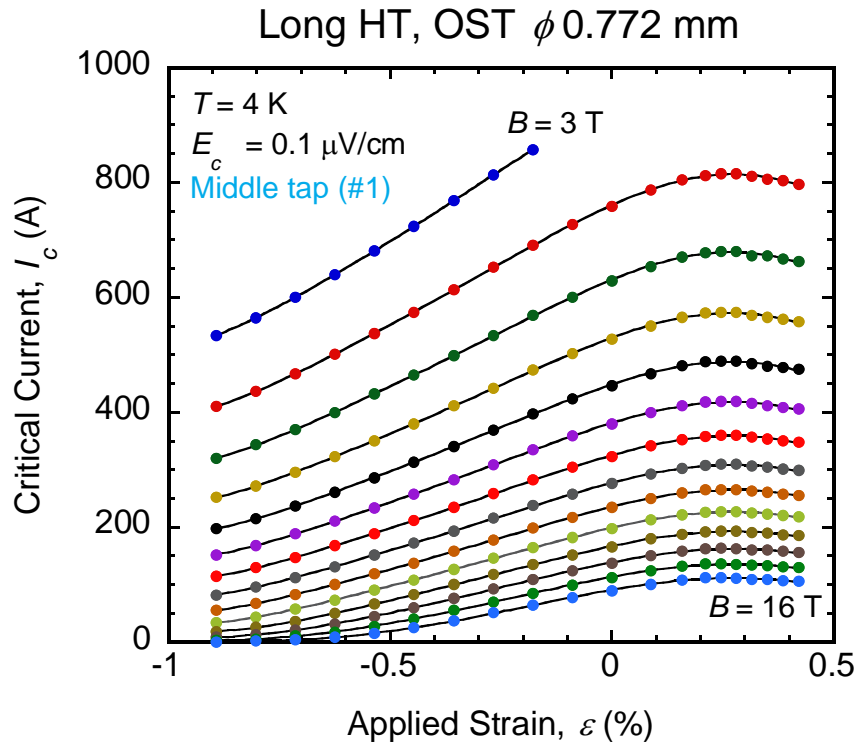


**Figure 11b: Critical-current (at 0.1 μV/cm) vs. strain and magnetic field at 4 K for an OST Nb₃Sn ITER wire (alternate design), heat-treated at 650 ˙C for 200 hours.**
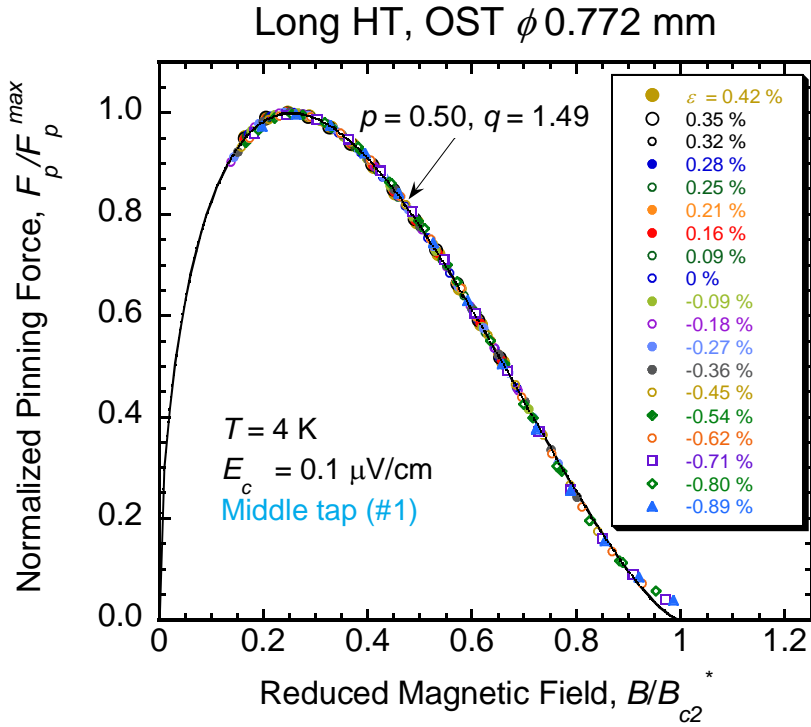
**Figure 12: Normalized pinning force vs. reduced magnetic field for an OST Nb$_3$Sn wire (alternate design), heat-treated at 650 ˚C for 200 hours. The pinning force scales with magnetic field for the various strain values that were applied to the sample.**
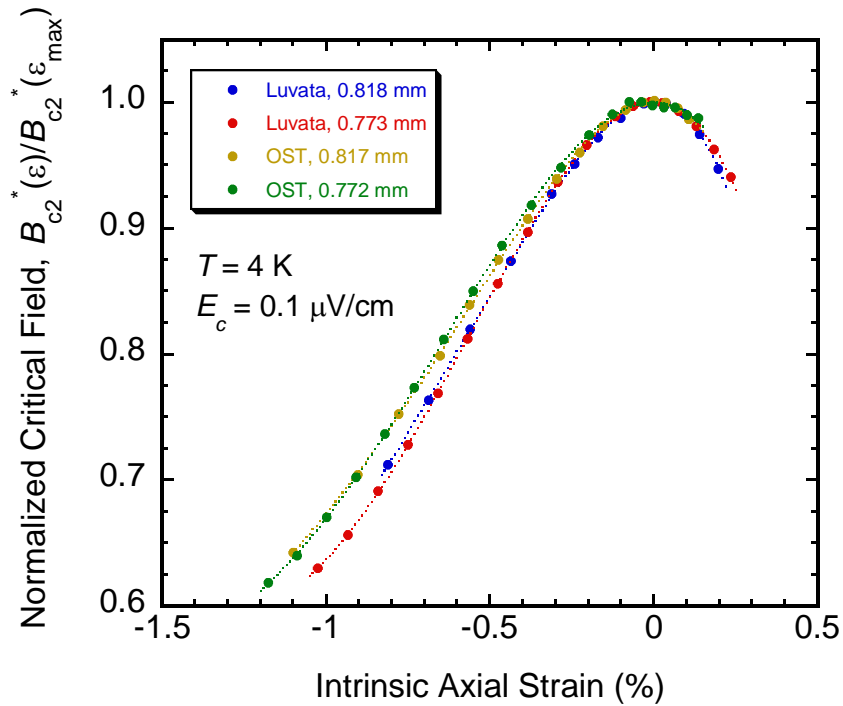


**Figure 13: Normalized critical field vs. intrinsic strain for Luvata and OST Nb$_3$Sn ITER wires. Luvata wires seem to be slightly more sensitive to high compressive strain as compared to OST strands. These wires may contain different ternary elements, or different effective amounts of the ternary elements in the Nb$_3$Sn.**

| | Luvata 0.818 mm | Luvata 0.773 mm | OST 0.817 mm | OST 0.772 mm |
|---|---|---|---|---|
| Heat Treatment | 650 °C 175 hours | 650 °C 175 hours | 650 °C 200 hours | 650 °C 200 hours |
| Tap | #3 | #3 | #3 | #1 |
| $p$ | 0.511 | 0.472 | 0.523 | 0.504 |
| $q$ | 1.486 | 1.537 | 1.514 | 1.485 |
| $B_{c2}^{*}{}_{max}$ (T) | 23.81 | 24.32 | 25.22 | 24.61 |
| $\varepsilon_{max}$ (%) | 0.31 | 0.30 | 0.30 | 0.29 |
| $c_2$ | -1.0946 | -0.9345 | -0.8903 | -0.7479 |
| $c_3$ | -1.1959 | -0.6922 | -0.8005 | -0.5109 |
| $c_4$ | -0.4767 | -0.1209 | -0.2366 | -0.0935 |

Table 3: List of the fitting parameters obtained for Luvata and OST Nb$_3$Sn ITER wires.

# REPORT OF ITER SERIES ROUND ROBIN TEST BY NIST IN 2009

## L. F. Goodrich and T. C. Stauffer

### National Institute of Standards and Technology
### Boulder, CO 80305

*Research Summary*

This report contains the measurement results from NIST on the ITER series round robin test that was completed in November 2009. The results are given on the standard ITER form for reporting critical current results.

# Annex A :   Heat Treatment Records

**HT Record Sheet ID:**   see CERN sample preparation for ITER Series Round Robin Test in 2009, samples mounted, heat-treated, and soldered by CERN

DA code            _____
Contact Person     _____
Affiliation        _____
Tel                __    , E-mail       _


Heat treatment Cycle is Cycle A    Yes _____ / No __

Table. 1    Temperature history

| | |
|---|---|
| | |

*)

# Annex B :    $I_c$ Test Results

DA code                    ___EU____                    , Sample ID-code __ _01BR8305A07C.020_

<div style="font-size:small">Name of institute / supplier</div>

Prepared at              ___CERN_____          , Tested at              ____NIST_____

Contact Person     ___Loren Goodrich_____
Affiliation               ___NIST_____
Tel                          ___303-497-3143_____   , E-mail                 ___goodrich@boulder.nist.gov_____

## Summary

Critical current  _191.4_ A at 12 T, _206.4_ A at 11.5 T and _177.3_ A at 12.5 T

(optional)

n-value                   _44.0_       at 12 T,   _43.9*_       at 11.5 T and   _43.2_    at 12.5 T

(optional)

Date of first cool down and final warm up            ___ ~ ____
Number of cool down and warm up cycles              ___1_____
Number of $I_c$ ramps                                         ___27_____
Heat treatment Cycle is Cycle A                          Yes ____ / No ___
Heat Treatment Record Sheet ID                          _CERN Round Robin 2009_

## $I_c$ Test Records

| Date-Time-Seq. | B (T) | Temp. (K) | Meas. $I_c$ (A) | $I_{c,Corr}$ at 4.22 K (A) | Meas. $I_c$ (A) with 0.25 m taps #1 / 2 | #2 / 2 | n-index | Comments |
|---|---|---|---|---|---|---|---|---|
| 11/18/2009-4:48 PM-06 | 12.5 | 4.224 | 177.1 | 177.2 | 177.4 | 176.9 | 43.1 | |
| 11/18/2009-4:50 PM-07 | 12.5 | 4.224 | 177.1 | 177.3 | 177.4 | 176.9 | 43.2 | |
| 11/18/2009-4:52 PM-08 | 12.5 | 4.224 | 177.2 | 177.3 | 177.4 | 176.9 | 43.3 | |
| 11/18/2009-4:57 PM-09 | 12 | 4.224 | 191.3 | 191.4 | 191.6 | 191.0 | 44.0 | |
| 11/18/2009-4:59 PM-10 | 12 | 4.224 | 191.3 | 191.4 | 191.6 | 191.0 | 44.0 | |
| 11/18/2009-5:02 PM-11 | 12 | 4.224 | 191.3 | 191.4 | 191.6 | 191.0 | 44.0 | |
| 11/18/2009-5:08 PM-12 | 11.5 | 4.224 | 206.3 | 206.4 | 206.6 | 206.0 | 43.9 | *n-index near 0.1 uV/cm |
| 11/18/2009-5:10 PM-13 | 11.5 | 4.224 | 206.3 | 206.4 | 206.6 | 206.0 | 43.9 | *n-index near 0.1 uV/cm |
| 11/18/2009-5:12 PM-14 | 11.5 | 4.224 | 206.3 | 206.4 | 206.6 | 206.0 | 43.9 | *n-index near 0.1 uV/cm |

$I_c$ procedure.

We used a ramp-and-hold current technique.

Measured $I_c$ of the 50 cm tap shown in column 4.

Note: One end of the sample (outside the center 50 cm) shows sign of lower Ic/damage and this limited the V-I curves at the lower fields.



2/4
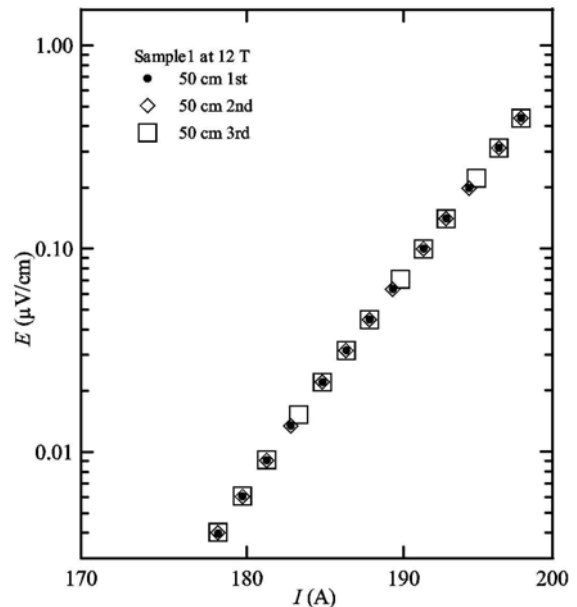
# Annex B :   $I_c$ Test Results

DA code                 ___EU____                  , Sample ID-code ___01BR8305A07C-026_

Name of institute / supplier

Prepared at          ___CERN_____          , Tested at          ____NIST_____

Contact Person     ___Loren Goodrich____
Affiliation          ___NIST_____
Tel                  ___303-497-3143_____     , E-mail          ___goodrich@boulder.nist.gov_____

**Summary**

        Critical current  _190.1_ A at 12 T, _205.0_ A at 11.5 T and _176.0_  A at 12.5 T
(optional)
        n-value              _43.4_     at 12 T,  _44.1_   at 11.5 T and  _42.7_   at 12.5 T
(optional)
            Date of first cool down and final warm up          __ ~ __
            Number of cool down and warm up cycles             ____1_____
            Number of $I_c$ ramps                              ____26_____
            Heat treatment Cycle is Cycle A                    Yes ____ / No ___
            Heat Treatment Record Sheet ID                     _CERN Round Robin 2009_

### $I_c$ Test Records

| Date-Time-Seq. | B (T) | Temp. (K) | Meas. $I_c$ (A) | $I_{c,Corr}$ at 4.22 K (A) | Meas. $I_c$ (A) with 0.25 m taps | | n-index | Comments |
|---|---|---|---|---|---|---|---|---|
| | | | | | #1 / 2 | #2 / 2 | | |
| 11/19/2009-2:46 PM-02 | 12.5 | 4.224 | 175.9 | 176.0 | 176.7 | 175.3 | 42.6 | |
| 11/19/2009-2:49 PM-03 | 12.5 | 4.224 | 175.9 | 176.0 | 176.7 | 175.2 | 42.7 | |
| 11/19/2009-2:51 PM-04 | 12.5 | 4.224 | 175.9 | 176.0 | 176.7 | 175.2 | 42.7 | |
| 11/19/2009-2:54 PM-05 | 12 | 4.224 | 190.0 | 190.1 | 190.8 | 189.3 | 43.4 | |
| 11/19/2009-2:57 PM-06 | 12 | 4.224 | 190.0 | 190.1 | 190.8 | 189.3 | 43.4 | |
| 11/19/2009-2:59 PM-07 | 12 | 4.224 | 190.0 | 190.1 | 190.8 | 189.2 | 43.4 | |
| 11/19/2009-3:02 PM-08 | 11.5 | 4.224 | 204.9 | 205.0 | 205.8 | 204.1 | 44.1 | |
| 11/19/2009-3:04 PM-09 | 11.5 | 4.224 | 204.9 | 205.0 | 205.8 | 204.1 | 44.1 | |
| 11/19/2009-3:06 PM-10 | 11.5 | 4.224 | 204.9 | 205.0 | 205.8 | 204.1 | 44.1 | |

$I_c$ procedure.

We used a ramp-and-hold current technique.

Measured $I_c$ of the 50 cm tap shown in column 4.



Sample2 at 12 T
• 50 cm 1st
◇ 50 cm 2nd
□ 50 cm 3rd
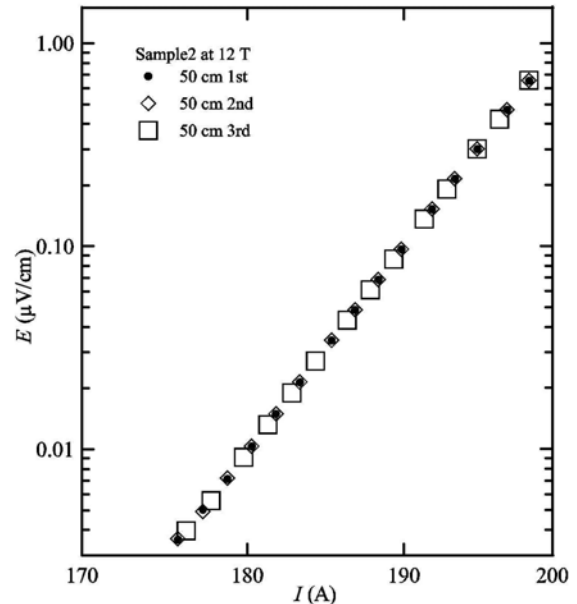
# Annex B :   $I_c$ Test Results

DA code ___EU____ , Sample ID-code __ 01BR8305A07C-037_

Name of institute / supplier

Prepared at ___CERN_____ , Tested at ____NIST_____

Contact Person ___Loren Goodrich____
Affiliation ___NIST_____
Tel ___303-497-3143_____ , E-mail ___goodrich@boulder.nist.gov_____

**Summary**

Critical current _190.1_ A at 12 T, _205.1_ A at 11.5 T and _176.1_ A at 12.5 T
(optional)

n-value _43.7_ at 12 T, _44.0_ at 11.5 T and _43.0_ at 12.5 T
(optional)

| | |
|---|---|
| Date of first cool down and final warm up | ____ ~ ___ |
| Number of cool down and warm up cycles | ____1_____ |
| Number of $I_c$ ramps | ____25_____ |
| Heat treatment Cycle is Cycle A | Yes ____ / No ____ |
| Heat Treatment Record Sheet ID | _ CERN Round Robin 2009 _ |

### $I_c$ Test Records

| Date-Time-Seq. | B (T) | Temp. (K) | Meas. $I_c$ (A) | $I_{c,Corr}$ at 4.22 K (A) | Meas. $I_c$ (A) with 0.25 m taps #1 / 2 | #2 / 2 | n-index | Comments |
|---|---|---|---|---|---|---|---|---|
| 11/20/2009-2:59 PM-02 | 12.5 | 4.221 | 176.1 | 176.1 | 176.0 | 176.1 | 42.9 | |
| 11/20/2009-3:01 PM-03 | 12.5 | 4.221 | 176.1 | 176.1 | 176.0 | 176.1 | 43.0 | |
| 11/20/2009-3:03 PM-04 | 12.5 | 4.221 | 176.1 | 176.1 | 176.0 | 176.1 | 43.0 | |
| 11/20/2009-3:10 PM-06 | 12 | 4.221 | 190.1 | 190.2 | 190.1 | 190.2 | 43.7 | |
| 11/20/2009-3:12 PM-07 | 12 | 4.221 | 190.1 | 190.1 | 190.1 | 190.2 | 43.7 | |
| 11/20/2009-3:14 PM-08 | 12 | 4.221 | 190.1 | 190.1 | 190.1 | 190.2 | 43.7 | |
| 11/20/2009-3:17 PM-09 | 11.5 | 4.221 | 205.1 | 205.1 | 205.0 | 205.1 | 44.3 | |
| 11/20/2009-3:19 PM-10 | 11.5 | 4.221 | 205.1 | 205.1 | 205.0 | 205.1 | 43.9 | |
| 11/20/2009-3:21 PM-11 | 11.5 | 4.221 | 205.1 | 205.1 | 205.0 | 205.1 | 43.9 | |

$I_c$ procedure.

We used a ramp-and-hold current technique.

Measured $I_c$ of the 50 cm tap shown in column 4.